Mechanical anisotropy and strain localization in textured zircaloy sheet

K.L.Murty, S.T.Mahmood & J.Talia
North Carolina State University, Raleigh, USA

1 INTRODUCTION

Zirconium alloys and other hexagonal close packed metals develop preferred orientations or textures during fabrication due mainly to the limited number of operating slip systems and the inherent anisotropy of the hexagonal single crystal. These textures are responsible for the anisotropy of properties exhibited by these materials. A knowledge of the mechanical anisotropy is required in predicting the dimensional changes of the fuel rods in service. Moreover, the mechanical anisotropy controls deep drawability through the formability parameter which dictates the ease with which zircaloy materials are fabricated into tubings from extrusions (Murty, 1985a). In addition, studies on the mechanical anisotropy of zircaloy sheets are important in the fabrication of grids in LWRs as well as channels in BWRs. The objective of the present study has been to characterize the deformation behavior, mechanical anisotropy and strain localization during tensile deformation of zircaloy sheet at ambient temperature. Recent advances in quantitative texture analyses and crystallite orientation distribution function (CODF) development in conjunction with appropriate crystal slip models made it possible to predict the multiaxial creep behavior, yield loci and formability characteristics of these materials (Murty 1985b).

2 EXPERIMENTAL DETAILS

Recrystallized zircaloy-4 sheets of 0.46mm thick were used for these studies and standard tensile specimens were fabricated with a gage length of 31.75mm and 6.35mm wide. These materials are typically used for channel and grid applications in water reactors. Zircaloy is the trade name given to zirconium alloyed with tin and iron, and has an hcp structure at service temperature with c/a ratio less than ideal. The specimens were machined with the tensile axis along the rolling and transverse directions and are referred to as the longitudinal (LT) and trasverse (TD) specimens respectively. Square grids of 1.27mm side were electrochemically etched on one of the surfaces to determine the strain distributions along the gage length and width as a function of the principal strain during uniform deformation proceeding through diffuse and local necking to fracture. The gridded side of the specimens was photographed at various times (strains) during deformation with a high resolution lens and the data were digitized for subsequent analyses.

Basal (00.1), prism (10.0)and pyramidal (10.2) pole figures were determined using direct pole figure method and are shown in Figure 1. RD and TD correspond to the rolling and transverse directions while the geometric center of each of the pole figures is the sheet normal. The basal pole peaks are noted at about 35° from the normal towards the transverse direction and the peaks in the prism poles occurred at 30° from the rolling direction towards the transverse direction. These are typical of the textures in recrystallized zirconium alloys.

3 CRYSTALLITE ORIENTATION DISTRIBUTION FUNCTION

The major drawback in the pole figure representation of preferred orientations is that two or more pole figures are needed to qualitatively recognize certain strong preferred orientations, the process which is qualitative in nature and could often be misleading. Quantitative representations of the textures is possible through an evaluation of a distribution function which gives the probability that a crystallite lies within a certain range of orientations with respect to the specified coordinates (generally processing axes). This function is called the orientation distribution function [CODF], $\omega(\theta,\psi,\phi)$, which expresses the probability that a crystallite has an orientation (θ,ψ,ϕ) with respect to the specimen axes (Bunge 1965; Roe 1965):

$$(1) \qquad \omega(\theta,\psi,\phi) = \sum_{l=0}^{\infty} \sum_{m=-1}^{1} \sum_{n=-1}^{1} W_{lmn} Z_{lmn}(\cos\theta) \exp(-im\psi) \exp(-in\phi)$$

where W_{lmn} are the appropriate series coefficients, Z_{lmn} are the augmented Jacobi polynomials and (θ,ψ,ϕ) are Euler angles (Figure 2) connecting coordinate axes embedded in the crystallite (O-XYZ) with axes coincident with the specimen and the principal working directions of the material (o-xyz). The CODF derived from the texture pole figures is often depicted as Euler plots (Figure 2) at fixed intervals of one of the angles (ϕ). Once the CODF is developed for a set of crystallographic texture pole figures, any orientation dependent property of a bulk polycrystal can be evaluated from single crystal data. Thus,

$$(3) \qquad \langle\rho(\theta,\psi,\phi)\rangle = \int_0^{2\pi}\int_0^{2\pi}\int_{-1}^{1} \rho(\theta,\psi,\phi)\, \omega(\theta,\psi,\phi)\, d(\cos\theta)\, d\psi\, d\phi$$

where $\rho(\theta,\psi,\phi)$ is the microscopic crystal property and $\langle\rho(\theta,\psi,\phi)\rangle$ the corresponding property of the textured polycrystalline aggregate. We assume here that the contribution of grain-to-grain interactions is negligible and thus it is deemed sufficient to weigh the property by the CODF in evaluating bulk behavior.

4 RESULTS AND DISCUSSION

Engineering and true stress-strain curves obtained from the fractured grid element of both the LT and TD specimens enabled an evaluation of

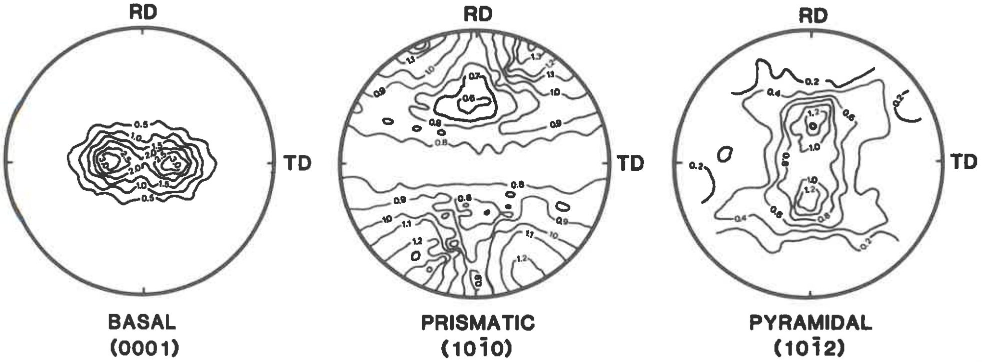

Figure 1. Crystallographic pole figures of recrystallized zircaloy-4 sheet.

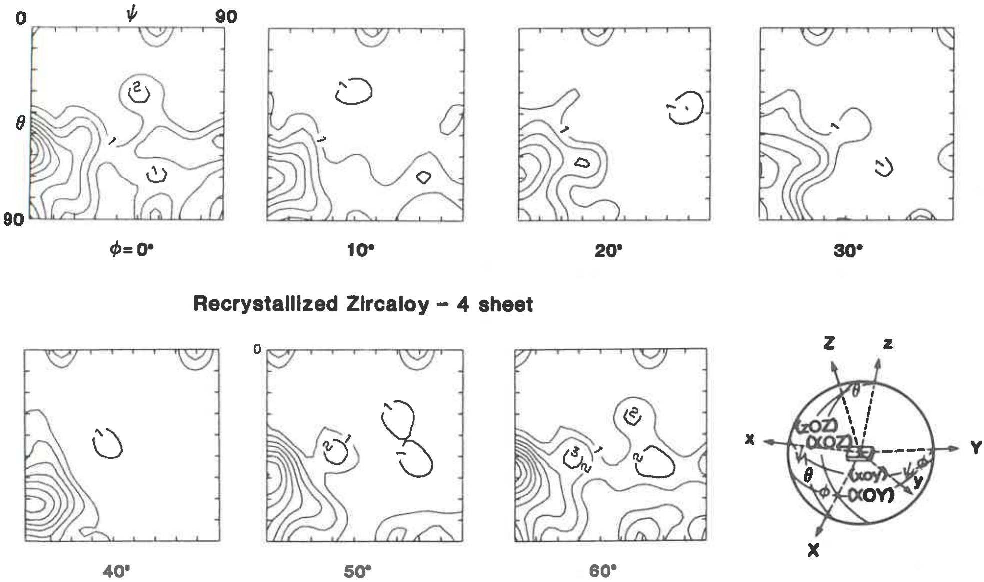

Figure 2. Euler plots representing the ODF of recrystallized zircaloy-4. The coordinate systems are shown in the bottom right-hand corner.

the various mechanical properties (Table 1). In the table 1, YS is the true yield stress, UTS the true tensile strength, n the work hardening parameter, ε_u the true strain in the neck upto maximum load representing the 'uniform' elongation, ε_c the critical strain for diffuse necking, ε_{ln} the limiting strain for local necking and ε_{fn} the true strain to fracture in the neck.

Table 1. Mechanical properties of zircaloy-4 sheet.

Specimen	YS MPa	UTS MPa	ε_u	n	ε_c	ε_{ln}	ε_{fn}
LT	289.4	392.7	0.15	0.14	0.09	0.79	0.83
TD	292.8	394.8	0.17	0.19	0.02	0.87	0.93

In addition to these mechanical characteristics, the grid analysis method enabled an evaluation of the transverse contractile strain-ratios (R and P) which are the mechanical anisotropy parameters in the modified von Mises - Hill formulation for the generalized yield behavior of anisotropic materials (Murty 1986). These anisotropy parameters were evaluated from the contractile versus tensile strains in the fractured grid elements in the LT and TD specimens. In both of these cases, we found that the transverse contractile strain varied linearly with the tensile strain upto fracture (>80% strain) while diffuse necking started at far lower strains (around 9% for TL and 2% for TD). These results indicate that triaxial stresses at the neck compensated for the texture rotation at these high strains. The strain independence of the transverse contractile strains, however, makes it relatively more convenient in modelling the plastic behaviors of these materials in practice. The contractile strain ratios along the rolling (R) and transverse directions (P) were close to each other but quite larger than unity (about 3.8) indicating that the material exhibits planar isotropy.

The mechanical anisotropy parameters can be used to evaluate the Backofen formability parameter (B) which is of importance in deep drawing and forming operations (Backofen 1972). The significance of the B parameter lies in the fact that the higher the B value of a given material the better are its formability characteristics. The main objective of the present investigation has been to attempt to incorporate CODF in an appropriate plasticity model to predict the mechanical anisotropy as well as the formability parameters.

4.1 MODEL PREDICTIONS

In evaluating the polycrystalline yield behavior, rigid body models such as Sachs, Taylor and Bishop-Hill are commonly used where specific slip systems are postulated to operate. One convenient method which comprises of the low and high temperature plasticity behaviors is to use a power law stress dependence of the strain-rate (Adams and Murty 1985):

$$(3) \quad \dot{\gamma}(k) = A \left\{ \frac{\tau(k)}{\tau_o(k)} \right\}^n$$

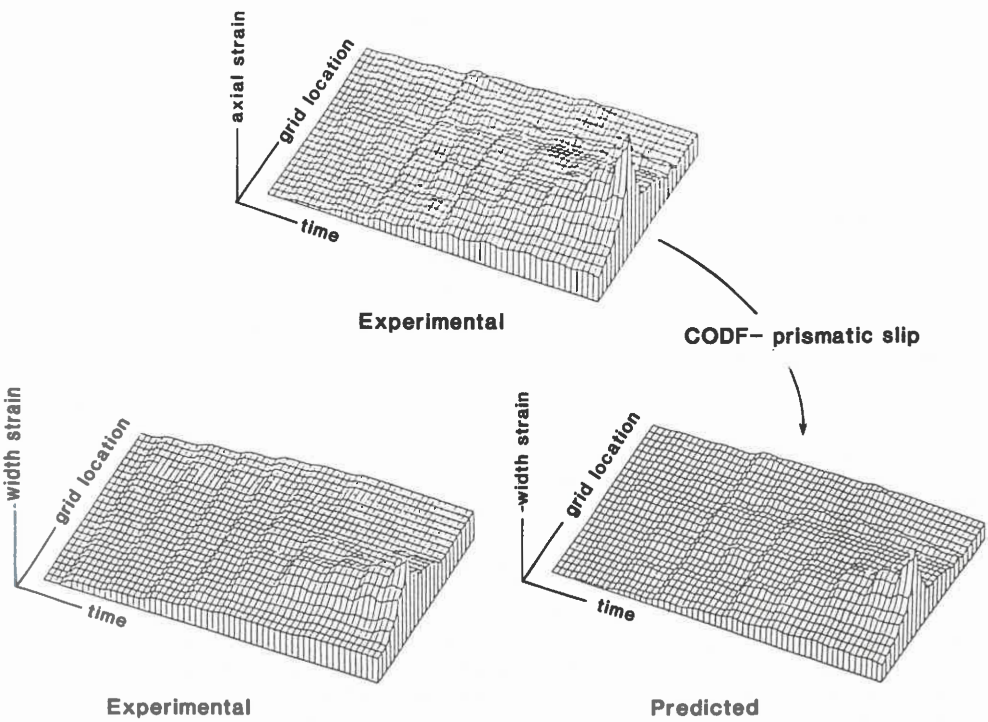

Figure 3. Spatial and temporal variations of tensile and contractile strains for recrystallized zircaloy-4 sheet (LT specimen).

where A is the reference strain-rate dependent on the test temperature and $\tau_0(k)$ is the reference shear stress prescribing the ease with which slip can occur on the kth plane. If the stress is regarded uniform throughout the bulk, a lower-bound estimate of the strain-rate is obtained from the CODF :

$$(4) \qquad \{\dot{\varepsilon}_{ij}\}_{\ell b} = \langle \dot{\varepsilon}_{ij} \rangle = \int_0^{2\pi} \int_0^{2\pi} \int_{-1}^{1} \omega(\theta,\psi,\phi)\ \dot{\varepsilon}_{ij}\ d(\cos\theta)\ d\psi\ d\phi$$

An analog of Voigt elastic upper-bound can be made by imposing the strain-rate perceived by the polycrystalline aggregate on each crystallite and evaluating the stress state in each crystallite. The uniform strain-rate upper-bound analysis converges to the rigid plastic behavior in the limit $n=\infty$ and recent calculations by Adams and Hirth (1981) revealed that such a behavior is approached at n values above about 50. We applied the CODF and crystal plasticity model to the sheet texture with n=100 which applies to ambient deformation where the strain-rate sensitivity is about 0.01. It is well known that low c/a ratio materials such as zirconium exhibit prism slip ($\{10.0\}\langle 11.0\rangle$) at low temperatures and both lower-bound and Bishop-Hill analyses were considered. The model predictions compared well with the experimental results (Table 2):

Table 2. Experimental and model predictions of R, P and B.

Parameter	Experimental	Model	
		Lower-Bound	Bishop-Hill
R	3.88±0.33	3.81	3.40
P	3.72±0.46	3.88	2.66
B	1.54	1.56	1.39

A more revealing correlation and the power of the model in predicting the anisotropic mechanical behavior are illustrated in Figure 3 where the predicted (based on lower-bound model) spatial and temporal variations of the transverse contractile strain are depicted along with the experimental data. It is also interesting to note that the lower-bound analysis gives much closer agreement with the experimental results whereas strain compatibility in the Bishop-Hill analysis is expected to model the real situation particularly at low temperatures. This is of significance since the Bishop-Hill analysis takes a relatively long computer time compared to lower-bound method.

This work was supported by the United States National Science Foundation under grant DMR-8313157.

REFERENCES

Adams, B.L. & J.P. Hirth 1981. The influence of texture and slip mode on creep constitutive behavior of hexagonal metals. In M.F.Ashby (ed.), Dislocation modelling of physical systems, p.368-372. New York: Pergamon.

Adams, B.L. & K.L. Murty 1985. Biaxial creep of textured zircaloy II: Crystal mean plastic modelling. Mat. Sci. Eng. 70:181-190.

Backofen, W.A. 1972. Deformation processing. Reading: Addison-Wesley.

Bunge, H.J. 1965. Zur darstellung allgemeiner texturen. Z. Metallkde. 56:872-874.

Murty, K.L. 1985a. Temperature and strain-rate dependences of mechanical anisotropy of zircaloy. In Proceedings of the 8th International conference on structural mechanics in reactor technology, p.C1/7. Amsterdam: Elsevier.

Murty, K.L. 1985b. Application of ODF in predicting creep and formability of textured metals. In Metals congress symposium on use of CODF for analysis of texture and prediction of properties, Toronto: ASM.

Murty, K.L. 1986. Biaxial creep of zircaloy cladding. Trans. I. I. M. 39:357-368.

Roe, R.J. 1965. Description of crystallite orientation in polycrystalline materials. III. General solution to pole figure inversion. J. Appl. Phys. 36:2024-2031.